Phase-field modeling of fracture in poroelastic solids for thermal energy storage

Xing-Yuan Miao[1,2], Olaf Kolditz[1,2], Thomas Nagel[1,3]

[1]Department of Environmental Informatics, Helmholtz Centre for Environmental Research – UFZ, Permoserstr. 15, 04318 Leipzig, Germany; PH (341) 235-1882; email: xing-yuan.miao@ufz.de
[2]Applied Environmental Systems Analysis, Technische Universität Dresden, Germany
[3]Department of Mechanical and Manufacturing Engineering, School of Engineering, Trinity College Dublin, College Green, Dublin, Ireland

ABSTRACT

The development of a continuum phase-field model of brittle fracture for poroelastic solids is presented. Three treatments for deriving the evolution equation of the phase-field are compared. The phase-field approach transforms the discontinuous crack interface into a continuous diffusive setting. The diffuseness is controlled by a length scale parameter which is also associated with the stress state in the process zone. A one-dimensional beam model with an analytical solution is provided for the verification of the current numerical implementation.

INTRODUCTION

The phase-field approach is a promising numerical treatment for addressing crack evolution. The principal highlight of this approach is to tackle the crack interface from a continuous configurational perspective. The fracture surfaces are no longer tracked and instead are represented by smooth phase transition boundaries that are interposed between the fully damaged and undamaged zones. The diffusive crack topology is characterised by a length scale parameter which also affects the stress state in the process zone. In the context of Γ-convergence, such a continuous diffusive crack converges to a discontinuous sharp crack with a Griffith-type surface energy.

The phase-field characterisation is proposed to patch the insufficient descriptions for the crack evolution in the framework of classical theory of brittle fracture. In this contribution, the specific motivation of exploring crack initiation and propagation in porous media comes from the observation of critical tensile stresses within a water-saturated material which is used in a novel thermal energy store, cf., Miao (2016), Miao (2017). Measurements on the material samples indicate that the material has a relatively low tensile strength and fails in a brittle manner.

Not only for this specific material, but also for other brittle storage materials, as well as geotechnical and geological materials, these critical stresses can cause damage and subsequently fracture which is associated with the partial loss of long-term mechanical stability of the structures they compose. Furthermore, the induced cracks can increase the permeability of the storage material and alter its water-retention properties. Driven by the purpose of providing a numerical implementation based on a general theoretical concept for various research projects, however, the main objective is to summarise a recent implementation into the open-source finite element platform OpenGeoSys, as well as different theoretical access routes to the topic.

NUMERICAL TREATMENT

Basic equations

In the framework of isotropic linear elasticity, the undamaged elastic energy density is

$$\psi_{\mathrm{e}}\left(\boldsymbol{\epsilon}_{\mathrm{el}}\right)=\frac{1}{2}\lambda\mathrm{tr}\left(\boldsymbol{\epsilon}_{\mathrm{el}}\right)^{2}+\mu\boldsymbol{\epsilon}_{\mathrm{el}}:\boldsymbol{\epsilon}_{\mathrm{el}} \tag{1}$$

where λ and μ are the Lamé constants.

The approximation of the Helmholtz free energy functional of a fractured body could have the formulation of

$$\begin{aligned}E\left(\boldsymbol{u},\mathrm{grad}\,\boldsymbol{u},d\right)=&\int_{\Omega}\left[\left(d^{2}+k\right)\psi_{\mathrm{e}}^{+}\left(\boldsymbol{\epsilon}_{\mathrm{el}}\right)+\psi_{\mathrm{e}}^{-}\left(\boldsymbol{\epsilon}_{\mathrm{el}}\right)\right]\mathrm{d}V\\&+g_{\mathrm{c}}\int_{\Omega}\left[\frac{1}{4\varepsilon}\left(1-d\right)^{2}+\varepsilon\mathrm{grad}\,d\cdot\mathrm{grad}\,d\right]\mathrm{d}V+\frac{1}{2\tau}\int_{\mathrm{CR}_{l-1}}d^{2}\mathrm{d}V\end{aligned} \tag{2}$$

where d represents the crack field, see, Fig. 1b; k represents a residual stiffness. A penalized functional is introduced as one of several options to prevent usually unphysical healing of the crack field with τ the penalty constant.

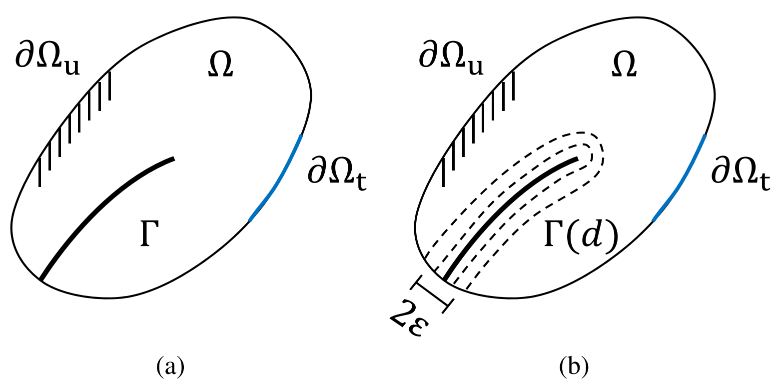

Figure 1: Elastic body with: (a) sharp crack; (b) diffusive crack characterised by a length scale parameter 2ε.

The external mechanical work functional is defined as

$$W_{\mathrm{ext}}\left(\boldsymbol{u}\right)=\int_{\partial\Omega_{\mathrm{t}}}\bar{\boldsymbol{t}}\cdot\boldsymbol{u}\mathrm{d}A+\int_{\Omega}\varrho\boldsymbol{b}\cdot\boldsymbol{u}\mathrm{d}V \tag{3}$$

where $\bar{\boldsymbol{t}}$ is the surface traction on $\partial\Omega_{\mathrm{t}}$, $\boldsymbol{b}$ the specific body force.

Thus, the global system assembles in the case of elastic deformation and brittle fracture

$$\Pi = E\left(\boldsymbol{u}, \operatorname{grad}\boldsymbol{u}, d\right) - W_{\mathrm{ext}}\left(\boldsymbol{u}\right), \tag{4}$$

with equilibrium for a quasi-static process demanding

$$\delta\Pi = \frac{\partial\Pi}{\partial\boldsymbol{u}}\cdot\delta\boldsymbol{u} + \frac{\partial\Pi}{\partial d}\delta d = 0 \tag{5}$$

Applying the Gauss theorem with respect to each term of the right-hand side of Eq. (5) yields

$$\begin{aligned}\frac{\partial\Pi}{\partial\boldsymbol{u}}\delta\boldsymbol{u} = &-\int_{\Omega}\operatorname{div}\left[\left(d^2+k\right)\boldsymbol{\sigma}_0^+ + \boldsymbol{\sigma}_0^-\right]\delta\boldsymbol{u}\mathrm{d}V + \int_{\partial\Omega_{\mathrm{t}}}\left[\left(d^2+k\right)\boldsymbol{\sigma}_0^+ + \boldsymbol{\sigma}_0^-\right]\boldsymbol{n}\cdot\delta\boldsymbol{u}\mathrm{d}A\\ &-\int_{\partial\Omega_{\mathrm{t}}}\bar{\boldsymbol{t}}\cdot\delta\boldsymbol{u}\mathrm{d}A - \int_{\Omega}\varrho\boldsymbol{b}\cdot\delta\boldsymbol{u}\mathrm{d}V\end{aligned} \tag{6}$$

$$\begin{aligned}\frac{\partial\Pi}{\partial d}\delta d = &\int_{\Omega}2d\psi_{\mathrm{e}}^+\left(\boldsymbol{\epsilon}_{\mathrm{el}}\right)\delta d\mathrm{d}V - \int_{\Omega}\frac{1-d}{2\varepsilon}g_{\mathrm{c}}\delta d\mathrm{d}V + \int_{\partial\Omega}2\varepsilon g_{\mathrm{c}}\operatorname{grad}d\cdot\boldsymbol{n}\delta d\mathrm{d}A\\ &-\int_{\Omega}2\varepsilon g_{\mathrm{c}}\operatorname{div}\left(\operatorname{grad}d\right)\delta d\mathrm{d}V + \frac{1}{\tau}\int_{\mathrm{CR}_{l-1}}d\delta d\mathrm{d}V\end{aligned} \tag{7}$$

thus leading to the following set of PDEs along with the respective Neumann-type boundary conditions

$$\operatorname{div}\left[\left(d^2+k\right)\boldsymbol{\sigma}_0^+ + \boldsymbol{\sigma}_0^-\right] + \varrho\boldsymbol{b} = \boldsymbol{0} \tag{8}$$

$$2d\psi_{\mathrm{e}}^+\left(\boldsymbol{\epsilon}_{\mathrm{el}}\right) - \frac{1-d}{2\varepsilon}g_{\mathrm{c}} - 2\varepsilon g_{\mathrm{c}}\operatorname{div}\left(\operatorname{grad}d\right) + \frac{d}{\tau}H\left(\epsilon_{\mathrm{tol}} - d\right) = 0 \tag{9}$$

$$\left[\left(d^2+k\right)\boldsymbol{\sigma}_0^+ + \boldsymbol{\sigma}_0^-\right]\cdot\boldsymbol{n} - \bar{\boldsymbol{t}} = \boldsymbol{0} \quad \text{on} \quad \partial\Omega_{\mathrm{t}} \tag{10}$$

$$\operatorname{grad}d\cdot\boldsymbol{n} = 0 \quad \text{on} \quad \partial\Omega \tag{11}$$

THREE APPROACHES OF DERIVING THE PHASE-FIELD EQUATION FOR NON-EQUILIBRIUM EVOLUTION

Thermodynamic formulation

Based on the first and second law of thermodynamics, in the framework of linear elasticity for small deformations, the Clausius-Planck inequality for an isothermal process in a purely mechanical setting with $\bar{\psi}\left(\boldsymbol{\epsilon}, d, \operatorname{grad}d\right)$ is formulated as (cf., Ehlers (2017))

$$\left(\boldsymbol{\sigma} - \varrho\frac{\partial\bar{\psi}}{\partial\boldsymbol{\epsilon}}\right) : \dot{\boldsymbol{\epsilon}} - \varrho\left[\frac{\partial\bar{\psi}}{\partial d} - \operatorname{div}\left(\frac{\partial\bar{\psi}}{\partial\operatorname{grad}d}\right)\right]\dot{d} - \varrho\operatorname{div}\left(\frac{\partial\bar{\psi}}{\partial\operatorname{grad}d}\dot{d}\right) \geq 0 \tag{12}$$

with a specific Helmholtz free energy $\bar{\psi}$. To fulfill the inequality, the constitutive equation for stresses is found as

$$\boldsymbol{\sigma} = \varrho\frac{\partial\bar{\psi}}{\partial\boldsymbol{\epsilon}} \tag{13}$$

and the boundary condition

$$\frac{\partial \bar{\psi}}{\partial \mathrm{grad}\, d} \cdot \boldsymbol{n} = 0 \quad \text{on} \quad \partial\Omega \tag{14}$$

The evolution equation can be found with $M > 0$ as

$$\dot{d} = -\varrho \left[\frac{\partial \bar{\psi}}{\partial d} - \mathrm{div} \left(\frac{\partial \bar{\psi}}{\partial \mathrm{grad}\, d} \right) \right] M \tag{15}$$

We here use a well-qualified approximating function proposed by Ambrosio (1990) to define the Helmholtz free energy functional as

$$\varrho \bar{\psi} = \left(d^2 + k \right) \psi_{\mathrm{e}}^{+} \left(\boldsymbol{\epsilon} \right) + g_{\mathrm{c}} \left[\frac{1}{4\varepsilon} \left(1 - d \right)^2 + \varepsilon \mathrm{grad}\, d \cdot \mathrm{grad}\, d \right] + \psi_{\mathrm{e}}^{-} \left(\boldsymbol{\epsilon} \right) \tag{16}$$

Substituting Eq. (16) into Eq. (15) obtains a specific formulation of the evolution equation

$$\frac{\dot{d}}{M} = -2d\psi_{\mathrm{e}}^{+} \left(\boldsymbol{\epsilon} \right) + g_{\mathrm{c}} \left[\frac{1}{2\varepsilon} \left(1 - d \right) + 2\varepsilon \mathrm{div} \left(\mathrm{grad}\, d \right) \right] \tag{17}$$

Geometrical treatment

A one-dimensional phase-field-type diffusive crack can be approached by an intuitive geometrical treatment, cf., Miehe (2010), see Fig. 1. The sharp crack (Fig. 1a) can be approximated by an exponential function

$$d(x) = 1 - \mathrm{e}^{\frac{-|x|}{2\varepsilon}} \tag{18}$$

with the Dirichlet-type boundary conditions

$$d(0) = 0 \quad \text{and} \quad d(\pm\infty) = 1 \tag{19}$$

Eq. (18) defines a diffusive crack topology (Fig. 1b). $\varepsilon \to 0$ implies that the diffusive crack converges to a discontinuous sharp crack. In a mathematical sense, it can be found that Eq. (18) is the solution of a second-order partial differential equation

$$4\varepsilon^2 d''(x) - d(x) + 1 = 0 \quad \text{in} \quad \Omega \tag{20}$$

Eq. (20) is the Euler equation of an integral with the solution

$$d = \underset{d \in \Lambda}{\mathrm{Arg\,min}} \left[I(d) \right] \tag{21}$$

with

$$I(d) = \Gamma_\varepsilon(d) = \int_\Omega \gamma \mathrm{d}V = \int_\Omega \left[\frac{1}{4\varepsilon} (1 - d)^2 + \varepsilon \mathrm{grad}\, d \cdot \mathrm{grad}\, d \right] \mathrm{d}V \tag{22}$$

where $\Lambda = \{ d | d(0) = 0, d(\pm\infty) = 1 \}$. The evolution of crack process is characterised by the extend of the regularised crack surface

$$\dot{\Gamma}_\varepsilon(d) = \int_\Omega \frac{\delta\gamma}{\delta d} \dot{d} \mathrm{d}V = \int_\Omega -\frac{1}{2\varepsilon} \left[(1 - d) + 2\varepsilon \mathrm{div} \left(\mathrm{grad} d \right) \right] \dot{d} \mathrm{d}V \geq 0 \tag{23}$$

Configurational forces

In the framework of isothermal phase transitions, the crack field d is treated as an order parameter characterising the phases of the body. The evolution of the crack field, i.e., the order parameter can be derived from the notion of configurational (material) forces. Gurtin (2008) introduced an additional configurational balance equation for the micro force system:

$$\mathrm{div}\boldsymbol{\xi} + \pi + \omega = 0 \tag{24}$$

Note that, in this context, $\boldsymbol{\xi}$ represents a micro stress vector, π and ω are scalar internal and external micro forces, respectively. Postulating $\tilde{\psi} = \tilde{\psi}\left(\boldsymbol{\epsilon}, d, \mathrm{grad}\, d, \dot{d}\right)$ the Clausius-Planck inequality extended for micro-system contributions reads

$$\left(\boldsymbol{\sigma} - \frac{\partial\tilde{\psi}}{\partial\boldsymbol{\epsilon}}\right) : \dot{\boldsymbol{\epsilon}} + \left(\boldsymbol{\xi} - \frac{\partial\tilde{\psi}}{\partial \mathrm{grad}\, d}\right) \cdot \mathrm{grad}\, \dot{d} - \left(\pi + \frac{\partial\tilde{\psi}}{\partial d}\right) \dot{d} - \frac{\partial\tilde{\psi}}{\partial \dot{d}} \ddot{d} \geq 0 \tag{25}$$

In which, due to equipresence, $\pi = \pi\left(\boldsymbol{\epsilon}, d, \mathrm{grad}\, d, \dot{d}\right)$. Then, the dissipation reads

$$\pi = -\frac{\dot{d}}{M} - \frac{\partial\tilde{\psi}}{\partial d} \tag{26}$$

Substituting Eq. (26) into Eq. (24) with $\omega := 0$ yields

$$\mathrm{div}\frac{\partial\tilde{\psi}}{\partial \mathrm{grad}\, d} - \frac{\partial\tilde{\psi}}{\partial d} = \frac{\dot{d}}{M} \tag{27}$$

Reformulating Eq. (27) based on Eq. (16) with respect to d, one obtains the Ginzburg-Landau-like evolution equation

$$\frac{\dot{d}}{M} = -2d\psi_{\mathrm{e}}\left(\boldsymbol{\epsilon}\right) + g_{\mathrm{c}}\left[\frac{1}{2\varepsilon}\left(1-d\right) + 2\varepsilon \mathrm{div}\left(\mathrm{grad}\, d\right)\right] \tag{28}$$

Note that all approaches lead to identical thermodynamically consistent results but highlight different conceptual perspectives.

NUMERICAL EXAMPLE

The numerical implementation into OpenGeoSys follows Gerasimov (2016) and is verified against a one-dimensional quasi-static beam model with an analytical solution stated in Kuhn (2013) to verify the phase-field implementation. A beam is stretched by a prescribed displacement load applied to its two tips, see, Fig. 2.

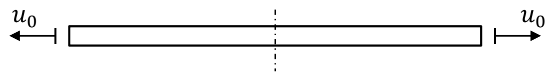

Figure 2: One-dimensional beam model.

Due to the symmetry of the boundary conditions, Fig. 3 only plots the phase-field parameter and displacement field distribution along a half beam. Comparisons of the analytical solution and the numerical approximation show the satisfactory match between these two solutions.

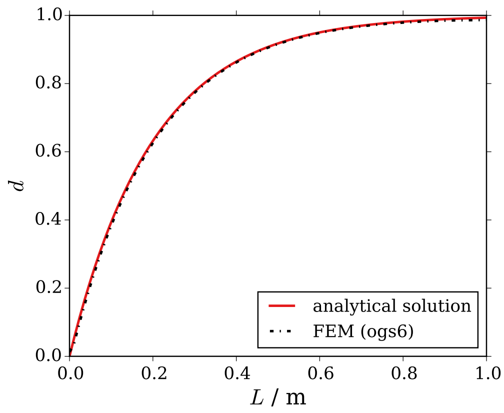

(a)

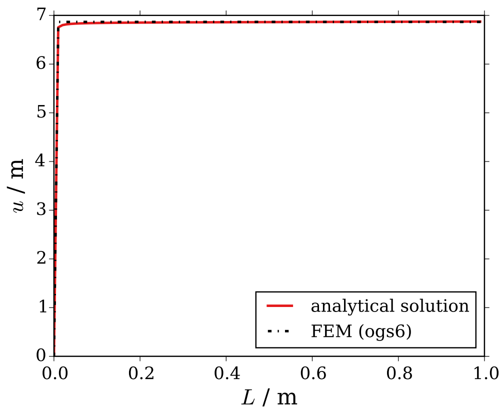

(b)

Figure 3: Phase-field parameter and displacement field distribution along the beam.

PHASE-FIELD MODELLING IN MULTI-PHYSICAL PROCESSES

To study how temperature and fluid-pressure fields affect the formation of cracks, and how the distribution of these field variables is affected by the presence of cracks, multi-physical aspects are incorporated into the framework. The thermo-hydraulic coupled phase-field approach is derived based on the Theory of Porous Media. Under the assumption of small deformations and brittle fracture, the Clausius-Planck inequality for the overall aggregate formulates, cf., Ehlers (2017),

$$\begin{aligned}
&\left(\boldsymbol{\sigma}_{\mathrm{S}} + \phi_{\mathrm{S}} p \mathbf{I} - \varrho_{\mathrm{S}} \frac{\partial \psi_{\mathrm{S}}}{\partial \boldsymbol{\epsilon}_{\mathrm{S}}}\right) : (\boldsymbol{\epsilon}_{\mathrm{S}})'_{\mathrm{S}} - \left(\varrho_{\mathrm{S}} \eta_{\mathrm{S}} - p \frac{\phi_{\mathrm{S}}}{\varrho_{\mathrm{SR0}}} \frac{\partial \varrho_{\mathrm{SR}}}{\partial T} + \varrho_{\mathrm{S}} \frac{\partial \psi_{\mathrm{S}}}{\partial T}\right) T'_{\mathrm{S}} \\
&+ (\boldsymbol{\sigma}_{\mathrm{F}} + \phi_{\mathrm{F}} p \mathbf{I}) : \mathbf{d}_{\mathrm{F}} - (\hat{\mathbf{p}}_{\mathrm{F}} - p \,\mathrm{grad}\, \phi_{\mathrm{F}}) \cdot \mathbf{w}_{\mathrm{F}} - \left(\varrho_{\mathrm{F}} \eta_{\mathrm{F}} - p \frac{\phi_{\mathrm{F}}}{\varrho_{\mathrm{FR0}}} \frac{\partial \varrho_{\mathrm{FR}}}{\partial T} + \varrho_{\mathrm{F}} \frac{\partial \psi_{\mathrm{F}}}{\partial T}\right) T'_{\mathrm{F}} \\
&- \varrho_{\mathrm{S}} \left[\frac{\partial \psi_{\mathrm{S}}}{\partial d_{\mathrm{S}}} - \mathrm{div}\left(\frac{\partial \psi_{\mathrm{S}}}{\partial \mathrm{grad}\, d_{\mathrm{S}}}\right)\right] (d_{\mathrm{S}})'_{\mathrm{S}} - \varrho_{\mathrm{S}} \mathrm{div}\left(\frac{\partial \psi_{\mathrm{S}}}{\partial \mathrm{grad}\, d_{\mathrm{S}}} (d_{\mathrm{S}})'_{\mathrm{S}}\right) \geq 0 \qquad (29)
\end{aligned}$$

where ϕ_{S} and ϕ_{F} represents the volume fraction for solid and fluid, respectively. $(\cdot)'_{\mathrm{S}} = \partial(\cdot)/\partial t + \mathrm{grad}\,(\cdot) \cdot \mathbf{v}_{\mathrm{S}}$ is the material time derivative of a quantity with respect to the solid motion. The extra solid and fluid stresses and entropy and the extra fluid momentum production are defined as

$$\boldsymbol{\sigma}^{\mathrm{E}}_{\mathrm{S}} = \boldsymbol{\sigma}_{\mathrm{S}} + \phi_{\mathrm{S}} p \mathbf{I}, \quad \boldsymbol{\sigma}^{\mathrm{E}}_{\mathrm{F}} = \boldsymbol{\sigma}_{\mathrm{F}} + \phi_{\mathrm{F}} p \mathbf{I} \qquad (30)$$

$$\eta^{\mathrm{E}}_{\mathrm{S}} = \eta_{\mathrm{S}} - \frac{p}{(\varrho_{\mathrm{SR}})^2} \frac{\partial \varrho_{\mathrm{SR}}}{\partial T}, \quad \eta^{\mathrm{E}}_{\mathrm{F}} = \eta_{\mathrm{F}} - \frac{p}{(\varrho_{\mathrm{FR}})^2} \frac{\partial \varrho_{\mathrm{FR}}}{\partial T} \qquad (31)$$

$$\hat{\mathbf{p}}^{\mathrm{E}}_{\mathrm{F}} = \hat{\mathbf{p}}_{\mathrm{F}} - p \,\mathrm{grad}\, \phi_{\mathrm{F}} \qquad (32)$$

To fulfill the inequality, the constitutive equation is found as

$$\boldsymbol{\sigma}^{\mathrm{E}}_{\mathrm{S}} = \varrho_{\mathrm{S}} \frac{\partial \psi_{\mathrm{S}}}{\partial \boldsymbol{\epsilon}_{\mathrm{S}}} \qquad (33)$$

and the boundary condition

$$\frac{\partial \psi_{\mathrm{S}}}{\partial \mathrm{grad}\, d_{\mathrm{S}}} \cdot \boldsymbol{n} = 0 \tag{34}$$

the non-equilibrium conditions, cf., Ehlers (2017)

$$\boldsymbol{\sigma}_{\mathrm{F}}^{\mathrm{E}} = 2\left(1 - d_{\mathrm{S}}\right)^{2} \phi_{\mathrm{F}} \mu_{\mathrm{FR}} \mathbf{d}_{\mathrm{F}} \tag{35}$$

$$\hat{\mathbf{p}}_{\mathrm{F}}^{\mathrm{E}} = -\left(d_{\mathrm{S}}\right)^{2}\left(\phi_{\mathrm{F}}\right)^{2} \mu_{\mathrm{FR}} \mathbf{K}_{\mathrm{S}}^{-1} \mathbf{w}_{\mathrm{F}} \tag{36}$$

as well as the evolution equation

$$\frac{\left(d_{\mathrm{S}}\right)_{\mathrm{S}}'}{M} = \varrho_{\mathrm{S}}\left[\frac{\partial \psi_{\mathrm{S}}}{\partial d_{\mathrm{S}}} - \mathrm{div}\left(\frac{\partial \psi_{\mathrm{S}}}{\partial \mathrm{grad}\, d_{\mathrm{S}}}\right)\right] \tag{37}$$

where μ_{FR} is the effective dynamic viscosity of the pore fluid, $\mathbf{K}_{\mathrm{S}}$ the intrinsic permeability. The Helmholtz free energy functions for solid and fluid phase are introduced as

$$\begin{aligned} \varrho_{\mathrm{S0}}\psi_{\mathrm{S}}\left(\boldsymbol{\epsilon}_{\mathrm{S}}, d_{\mathrm{S}}, \mathrm{grad}\, d_{\mathrm{S}}, T\right) = {} & \left[\left(d_{\mathrm{S}}\right)^{2} + k\right]\left(\psi_{\mathrm{Se}}\right)^{+}\left(\boldsymbol{\epsilon}_{\mathrm{S}}\right) + \left(\psi_{\mathrm{Se}}\right)^{-}\left(\boldsymbol{\epsilon}_{\mathrm{S}}\right) \\ & - 3\alpha_{T\mathrm{S}} K_{\mathrm{S}}\left(T - T_{\mathrm{S0}}\right)\boldsymbol{\epsilon}_{\mathrm{S}} : \mathbf{I} + g_{\mathrm{Sc}}\left[\frac{1}{4\varepsilon}\left(1 - d_{\mathrm{S}}\right)^{2} + \varepsilon \mathrm{grad}\, d_{\mathrm{S}} \cdot \mathrm{grad}\, d_{\mathrm{S}}\right] \\ & - \varrho_{\mathrm{S0}} c_{\mathrm{S}}^{\mathrm{E}}\left(T \ln\frac{T}{T_{\mathrm{S0}}} - T + T_{\mathrm{S0}}\right) - \varrho_{\mathrm{S0}}\eta_{\mathrm{S0}}\left(T - T_{\mathrm{S0}}\right) \end{aligned} \tag{38}$$

$$\varrho_{\mathrm{F0}}\psi_{\mathrm{F}}\left(T\right) = -\varrho_{\mathrm{F0}} c_{\mathrm{F}}^{\mathrm{E}}\left(T \ln\frac{T}{T_{\mathrm{F0}}} - T + T_{\mathrm{F0}}\right) - \varrho_{\mathrm{F0}}\eta_{\mathrm{F0}}\left(T - T_{\mathrm{F0}}\right) \tag{39}$$

The governing partial differential equations read (cf., Ehlers (2017))
Mixture volume balance:

$$\mathrm{div}\left(\mathbf{v}_{\mathrm{S}} + \phi_{\mathrm{F}}\mathbf{w}_{\mathrm{F}}\right) - \left(\phi_{\mathrm{S}} 3\alpha_{T\mathrm{S}} + \phi_{\mathrm{F}}\beta_{T\mathrm{F}}\right)\left(T\right)_{\mathrm{S}}' - \phi_{\mathrm{F}}\beta_{T\mathrm{F}} \mathrm{grad}\, T \cdot \mathbf{w}_{\mathrm{F}} = 0 \tag{40}$$

Momentum balance for solid phase:

$$\varrho_{\mathrm{S}}\left(\mathbf{v}_{\mathrm{S}}\right)_{\mathrm{S}}' = \mathrm{div}\boldsymbol{\sigma}_{\mathrm{S}}^{\mathrm{E}} - \phi_{\mathrm{S}} \mathrm{grad}\, p + \varrho_{\mathrm{S}}\boldsymbol{g} - \hat{\mathbf{p}}_{\mathrm{F}}^{\mathrm{E}} \tag{41}$$

Momentum balance for fluid phase:

$$\varrho_{\mathrm{F}}\left(\mathbf{v}_{\mathrm{F}}\right)_{\mathrm{F}}' = \mathrm{div}\boldsymbol{\sigma}_{\mathrm{F}}^{\mathrm{E}} - \phi_{\mathrm{F}} \mathrm{grad}\, p + \varrho_{\mathrm{F}}\boldsymbol{g} - \hat{\mathbf{p}}_{\mathrm{F}}^{\mathrm{E}} \tag{42}$$

Mixture energy balance:

$$\left(\varrho c_{p}\right)_{\mathrm{eff}} \frac{\partial T}{\partial t} + \phi_{\mathrm{F}}\varrho_{\mathrm{FR}} c_{p\mathrm{F}} \mathrm{grad}\, T \cdot \mathbf{w}_{\mathrm{F}} - \mathrm{div}\left(\boldsymbol{\lambda}_{\mathrm{eff}} \mathrm{grad}\, T\right) = 0 \tag{43}$$

Evolution equation for phase-field:

$$\frac{\left(d_{\mathrm{S}}\right)_{\mathrm{S}}'}{M} = 2 d_{\mathrm{S}}\left(\psi_{\mathrm{S}e}\right)^{+}\left(\boldsymbol{\epsilon}_{\mathrm{S}}\right) + g_{\mathrm{S}c}\left[\frac{1}{2\varepsilon}\left(1 - d_{\mathrm{S}}\right) + 2\varepsilon \mathrm{div}\left(\mathrm{grad}\, d_{\mathrm{S}}\right)\right] \tag{44}$$

CONCLUSION

In this contribution, a continuum phase-field model of brittle fracture was presented. To offer physical insight to the interested reader, three treatments for obtaining the evolution equation of the phase-field were summarised. The direct incentive of developing a phase-field model is to allow the assessment for the crack formation and evolution in porous storage material under multi-physical conditions. The model implementation was outlined and the pure mechanical case was verified through comparing with an analytical solution.

REFERENCES

Ambrosio, L., Tortorelli, V. M., 1990. Approximation of functional depending on jumps by elliptic functional via t-convergence. Communications on Pure and Applied Mathematics 43 (8), 9991036.

Ehlers, W., Luo, C., 2017. A phase-field approach embedded in the theory of porous media for the description of dynamic hydraulic fracturing. Computer Methods in Applied Mechanics and Engineering 315, 348368.

Gerasimov, T., De Lorenzis, L., 2016. A line search assisted monolithic approach for phase-field computing of brittle fracture. Computer Methods in Applied Mechanics and Engineering 312, 276303.

Gurtin, M. E., 2008. Configurational forces as basic concepts of continuum physics. Vol. 137. Springer Science & Business Media.

Kuhn, C., 2013. Numerical and analytical investigation of a phase field model for fracture. Ph.D. thesis, Technische Universitt Kaiserslautern.

Miao, X.-Y., Beyer, C., Grke, U.-J., Kolditz, O., Hailemariam, H., Nagel, T., 2016. Thermo-hydro-mechanical analysis of cement-based sensible heat stores for domestic applications. Environmental Earth Sciences 75 (18), 1293.

Miao, X.-Y., Zheng, T., Grke, U.-J., Kolditz, O., Nagel, T., 2017. Thermo-mechanical analysis of heat exchanger design for thermal energy storage systems. Applied Thermal Engineering 114, 1082-1089.

Miehe, C., Welschinger, F., Hofacker, M., 2010. Thermodynamically consistent phase-field models of fracture: Variational principles and multi-field fe implementations. International Journal for Numerical Methods in Engineering 83 (10), 12731311.